

## Nanoparticles with Individual Site-Isolated Semiconducting Polymers from Intramolecular Chain Collapse Processes

Chinessa T. Adkins, Hubert Muchalski, and Eva Harth\*

*Department of Chemistry, 7619 Stevenson Center, Vanderbilt University, Nashville, Tennessee 37235*

*Received April 10, 2009; Revised Manuscript Received June 17, 2009*

**ABSTRACT:** We present the synthesis of polymeric nanoparticles from single ABA type block copolymers in an intramolecular-chain process to result 3-D architectures that confine a single chain of conducting copolymers. ABA triblock copolymers were prepared from conducting polymers such as fluorene homopolymers and fluorene/thiophene copolymers designed as telechelic macroinitiators to facilitate nitroxide-mediated living free radical polymerization methods. The polymerization with styrene and vinylbenzofluorene cross-linking units led to the desired ABA triblock copolymers with 8:1:8 and 5:1:5 ratios of the polymer copolymer blocks under living free radical polymerization conditions. In an intramolecular chain collapse process the ABA triblock copolymers form well-defined single chain nanoparticles with the confined semiconducting polymer block as core unit via a controlled cross-linking of the benzofluorene unit in the A block copolymer. The photoluminescence measurements illustrate the influence of the molecular weight of the A block to be crucial for the site isolation of the embedded conducting polymer block in the resulting nanoparticles with increased quantum efficiencies of 6%.

### Introduction

Inorganic quantum dots have developed to highly desirable building blocks for the construction of optoelectronic materials and devices.<sup>1–5</sup> Intriguing properties of narrow luminescence profiles and well-defined dimensions have been the motivation to create equivalent materials based on organic building blocks to overcome limitations of costly preparations and toxicities *in vivo*. Currently, attractive fluorescent materials are discovered as photostable biological imaging reagents and found entry into life science applications.<sup>6–10</sup> For example, linear semiconducting polymers such as poly(*p*-phenylene ethynylene) have been modified with polyvalent synthetic ligands as nonspecific low-affinity binding elements for the selective recognition of the extracellular matrix protein fibronectin.<sup>11</sup> In a similar approach, highly fluorescent perylene derivatives are implemented as core units with attached hydrophilic polyacrylate arms to compose fluorescent core–shell nanoparticles that localize in the nucleus of cells.<sup>12</sup> The positively charged counterparts with integrated amine groups in the shell forming polymer arms were utilized in the imaging of extracellular matrices.<sup>13</sup> Furthermore, the confinement of small molecule dyes in inorganic matrices such as silica particles (C-dots) are studied as fluorescent labels where the protected fluorescent core is key to the more stable imaging entity and underline the vast variety and utility of fluorophore components and organic structures known today.<sup>14,15</sup>

So far we did not discuss 3-D architectures that are solely made from conducting polymers serving as structural and emitting entities with unique electrooptical properties being employed. Approaches to confine conjugated polymers into a 3-D architecture range from miniemulsion methods to form submicrometer-sized conjugated particles composed of multiple copies of polymer chains<sup>16,17</sup> to nanoprecipitation methods to yield particles in size dimensions of 5–30 nm.<sup>18–20</sup> The observed nontoxicity and photostability makes these materials attractive as reagents in live cell imaging as alternatives to inorganic quantum dots. In many

of these strategies, the nanoparticle formation is the result of precipitation methods and leads to supramolecular structures that are not permanent for postmodification reactions performed in organic solutions. To further advance the field of organic, fluorescence-based nanoparticles, it will be necessary to develop techniques that afford stable, well-defined structures to allow a broader range of manipulations. With the goal to design stable supramolecular structures, we aimed for techniques that confine individual polymer molecules in one nanostructure to give controlled sizes equivalent to inorganic quantum dots and use the site isolation of the individual polymers as means to influence the electrochemical and physical processes in conducting polymers.

In this work, we present the formation of stable organic conjugated nanoparticles that are comprised from a single polymeric precursor utilizing an intramolecular chain collapse process. The two key elements of the linear conjugated precursors involved the design of an ABA triblock copolymer with incorporated cross-linking units in the A block copolymers to site-isolate the embedded semiconducting core block and form distinctive well-defined particles in nanoscopic dimensions of 5–10 nm. The increased photoluminescence is a direct measure of the efficiency in the confinement of the semiconducting block depending on the length of the A block copolymers and represents the first example of cross-linked nanoparticles from individual polymer chains as a result of the intramolecular chain collapse technique.

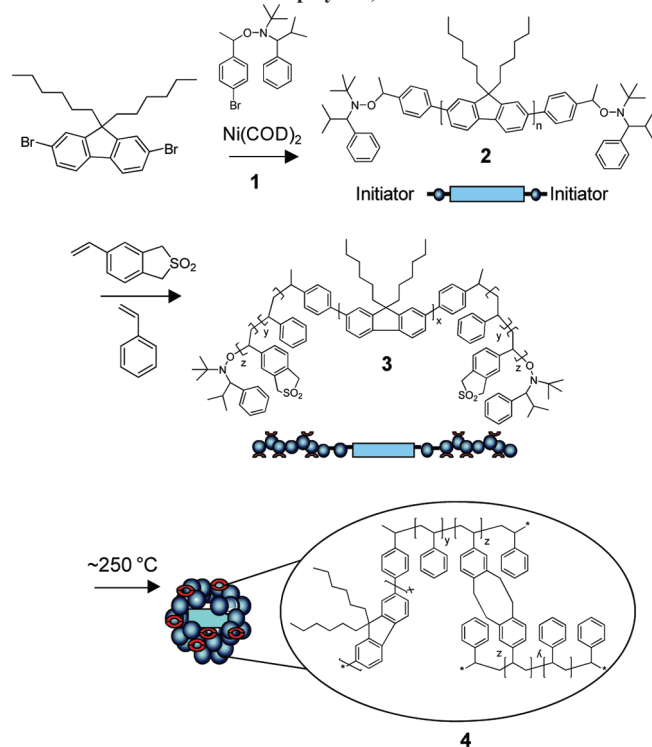
### Experimental Section

Analytical thin layer chromatography (TLC) was carried out on commercial Merck plates coated with silica gel GF254 (0.24 mm). Column chromatography was carried out with Merck silica gel, 230–400 mesh. NMR spectra ( $\delta$ , ppm) were recorded on a 400 MHz FT-NMR spectrometer at ambient temperature. All spectra were recorded in CDCl<sub>3</sub>, and the resonances were measured relative to residual solvent. Weight-average ( $M_w$ ) molecular weights relative to linear polystyrene and polydispersity indices ( $PDI = M_w/M_n$ ) were determined by gel permeation chromatography (GPC) at ambient temperature using tetrahydrofuran

\*Corresponding author. E-mail: eva.harth@vanderbilt.edu.

(THF) as solvent (1.0 mL/min), a set of  $10^2$ ,  $10^3$ ,  $10^5$ ,  $10^6$  Å Styragel 5  $\mu$ m columns, a Waters 410 differential refractometer, and Millenium Empower 2 software. Particle size and absolute molecular weights were determined by dynamic light scattering (DLS) and static light scattering (SLS), respectively, on a Zetasizer Nano Series instrument at 25 °C with a CGS-3 compact goniometer system by Malvern Instruments equipped with a vertically polarized 35 mW He–Ne 633 laser with samples dissolved in dichloromethane. All samples were dissolved overnight, filtered through a 0.45  $\mu$ m filter, and run at a fixed 90° angle with the light wavelength at 690 nm. The values of refractive index increment ( $dn/dc$ ) for star polymers were

**Scheme 1. Synthesis of Single-Chain Nanoparticles from ABA Block Copolymer, 2**



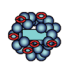


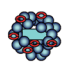


measured in THF at 25 °C by using a refractometer. UV–visible (UV–vis) absorption spectra were obtained with a Varian Cary 50 spectrophotometer in dichloromethane. Photoluminescence spectra were taken on an ISS PCI photon counting spectrofluorometer in dichloromethane. Fluorescence quantum yields ( $\Phi_f$ ) were determined relative to 9,10-diphenylanthracene in dichloromethane ( $\Phi = 0.9$ ) as the standard. Morphology of the polymer blend nanoparticles were characterized by atomic force microscopy (AFM). For the AFM measurements, the nanoparticle solution was spin-coated onto an oxidized silicon wafer. The surface was scanned with a Digital Instruments multimode AFM in tapping mode. Olympus cantilevers, with a spring constant of 42 N/m, resonating at 300 kHz, have been used for all measurements.

**Materials.** 9,9'-Dihexyl-2,7-dibromofluorene (Aldrich, 97%), 2,5-dibromo-3-hexylthiophene (Aldrich, 97%), styrene (Acros, 99%), 4-bromostyrene (Aldrich, 98%), Jacobsen's reagent (Acros, 98%), and sodium borohydride (Acros, 98%) were used as received. *N-tert*-Butyl- $\alpha$ -isopropyl nitroxide,<sup>21</sup> 2,2,5-trimethyl-4-phenyl-3-azahexane-3-nitroxide,<sup>21</sup> and vinylbenzotriazole<sup>22</sup> were prepared as described previously. All solvents were commercially available and used as received.

**4-Bromophenyl-2,2,5-trimethyl-2-(1-phenylethoxy)-3-azahexane, 1.** A mixture of 150 mL of toluene and 150 mL of ethanol was bubbled with air for 1 h, after which 2,2,5-trimethyl-4-phenyl-3-azahexane-3-nitroxide (7.10 g, 32.2 mmol), 4-bromostyrene (8.85 g, 47.2 mmol), Jacobsen's reagent (4.22 g, 6.64 mmol), and sodium borohydride (4.52 g, 120 mmol) were added to the solvents. Air was bubbled through the mixture for 4 h, and the reaction was allowed to stir overnight. The mixture was then filtered through a glass frit and washed with methylene chloride, ethanol, and methanol. The filtrate was then collected and concentrated in vacuo to give a brown viscous liquid. The bromo  $\alpha$ -alkoxyamine initiator was purified by flash column chromatography (10:1 hexanes/ethyl acetate) to give the title compound as a clear oil (5.20 g, 73.2%). <sup>1</sup>H NMR (400 MHz, CDCl<sub>3</sub>,  $\delta$ ): 7.05–7.40 (m, 9H, ArH), 4.75 (m, 1H, CH), 3.21 (d,  $J = 9.3$  Hz, 1H, CH), 2.20 (m, 1H, CH), 1.62 (d,  $J = 6.5$  Hz, 3H, CH<sub>3</sub>), 1.54 (s, 9H, CH<sub>3</sub>), 0.92 (d,  $J = 6.5$  Hz, 6H, CH<sub>3</sub>). <sup>13</sup>C NMR (100 MHz, CDCl<sub>3</sub>,  $\delta$ ): 144.50 (C), 140.12 (C), 132.12 (C), 129.22 (CH), 128.23 (CH), 127.90 (CH), 125.82 (CH), 123.12 (CH), 80.22 (CH), 73.23 (CH), 71.25 (C), 29.40 (CH), 27.42 (CH<sub>3</sub>), 19.35 (CH<sub>3</sub>), 18.10 (CH<sub>3</sub>).

**Table 1. Characterization Data for Semiconducting Macroinitiator, Linear Precursor, and Nanoparticles**

| Symbol  | Compound Number | Molecular Weight Ratio | $M_w$ , NMR (g/mol) | $M_w$ , theoretical (g/mol) | $M_w$ , RI (g/mol) <sup>a</sup> | PDI <sup>b</sup> |
|---|-----------------|------------------------|---------------------|-----------------------------|---------------------------------|------------------|
| Initiator—  —Initiator | 2               | —                      | 6600                | —                           | 1600                            | 4.7              |
|                        | 3               | 8:1:8                  | 106000              | 106000                      | 143000                          | 2.4              |
|                        | 4               | —                      | —                   | —                           | 99000                           | 2.0              |
| Initiator—  —Initiator | 5               | —                      | 6700                | —                           | 3800                            | 6.0              |
|                        | 6               | 5:1:5                  | 70000               | 75000                       | 39000                           | 4.8              |
|                        | 7               | —                      | —                   | —                           | 74000                           | 2.1              |

<sup>a</sup> Weight-average molecular weight ( $M_w$ ) after purification; gel permeation chromatography (GPC) data relative to PS standards. <sup>b</sup> Polydispersity ( $PDI = M_w/M_n$ ), measured by gel permeation chromatography (GPC) with tetrahydrofuran as eluent and integrated RI detector; calibration with linear PS as standard.

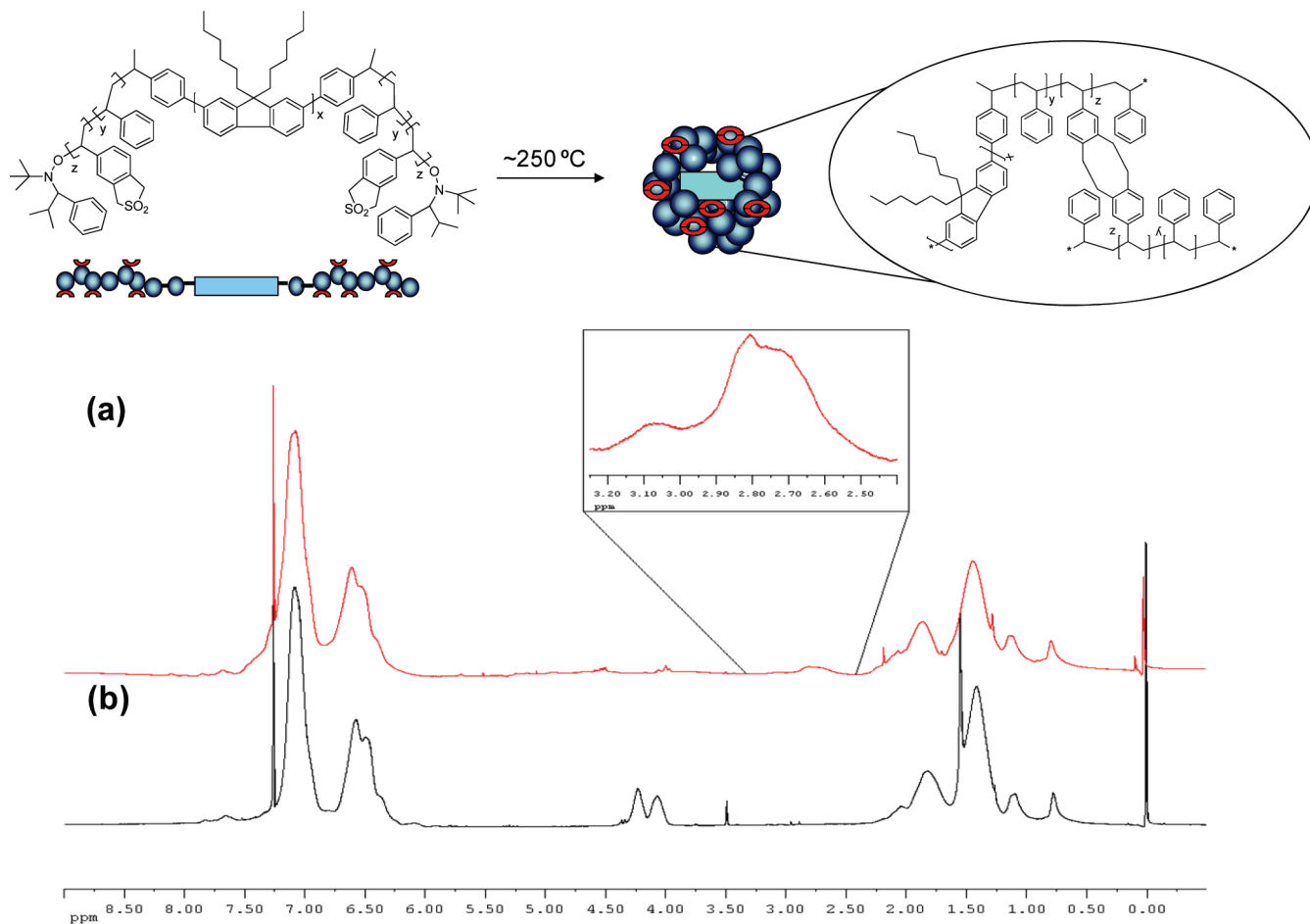


**Figure 1.**  $^1\text{H}$  NMR spectra of (a) fluorene linear precursor, **3**, and (b) fluorene nanoparticle, **4**.

**Synthesis of Fluorene Macromolecular Initiator, **2**.** A 100 mL three-neck round-bottom flask containing bis(1,5-cyclooctadiene)-nickel(0) (0.70 g, 2.5 mmol), 2,2'-bipyridyl (0.45 g, 2.90 mmol), 1,5-cyclooctadiene (0.2 mL), dry DMF (6 mL), and dry toluene (6 mL) was heated under argon to 80 °C for 30 min. Then 9,9'-dihexyl-2,7-dibromofluorene (0.55 g, 1.13 mmol) and **1** (0.16 g, 0.39 mmol) dissolved in 6 mL of degassed toluene were added under argon to the dark blue reaction mixture. After heating for 24 h in the dark, the hot polymer solution was precipitated into 600 mL of a 1:1:1 solution of HCl:acetone:MeOH. After isolating the crude product via filtration, the bromo-substituted  $\alpha$ -alkoxyamine-capped polymer was dissolved in dichloromethane (5 mL) and reprecipitated into a mixture of 440 mL of an acetone:MeOH solution for further purification (1.05 g, 91.3%,  $M_w = 1600$ , PDI = 4.7).  $^1\text{H}$  NMR (400 MHz,  $\text{CDCl}_3$ ,  $\delta$ ): 7.45–7.8 (m, ArH), 2.05 (br s,  $\text{CH}_2$ ), 1.90 (m,  $\text{CH}_2$ ), 1.28 (br s,  $\text{CH}_2$ ), 1.20 (s,  $\text{CH}_2$ ), 1.03 (br s,  $\text{CH}_2$ ), 0.62 (br s,  $\text{CH}_3$ ).  $^{13}\text{C}$  NMR (100 MHz,  $\text{CDCl}_3$ ,  $\delta$ ): 148.3, 147.7, 139.9, 138.0, 134.0, 132.0, 130.5, 128.5, 124.5, 123.0, 122.3, 122.1, 50.3, 43.9, 40.1, 31.8, 29.9, 24.4, 14.7.

**Fluorene Linear Precursor, **3**.** A mixture of **2** (0.10 g, 0.06 mmol,  $M_w = 1600$  (GPC), PDI = 4.7), styrene (1.47 g, 14.1 mmol), and vinylbenzofluorene (0.30 g, 1.54 mmol) dissolved in 1,2-dichlorobenzene (1.0 mL) was degassed by three freeze/pump/thaw cycles, sealed under argon, and heated at 124 °C for 16 h. The viscous reaction mixture was then allowed to cool, dissolved in dichloromethane (10 mL), and precipitated into methanol (1000 mL). The purified polymer was collected by vacuum filtration and dried to give the ABA triblock copolymer, polystyrene–poly(fluorene)–polystyrene as an off-white solid (1.21 g, 86.4% yield,  $M_w = 143\,000$  (GPC), PDI = 2.4,  $\Phi_f = 2.9\%$ ).  $^1\text{H}$  NMR (400 MHz,  $\text{CDCl}_3$ ,  $\delta$ ): 7.28–7.65 (m, ArH from poly(fluorene)), 6.22–7.20 (m, ArH, from poly(styrene) and poly(fluorene)), 3.97–4.25 (br m, CH

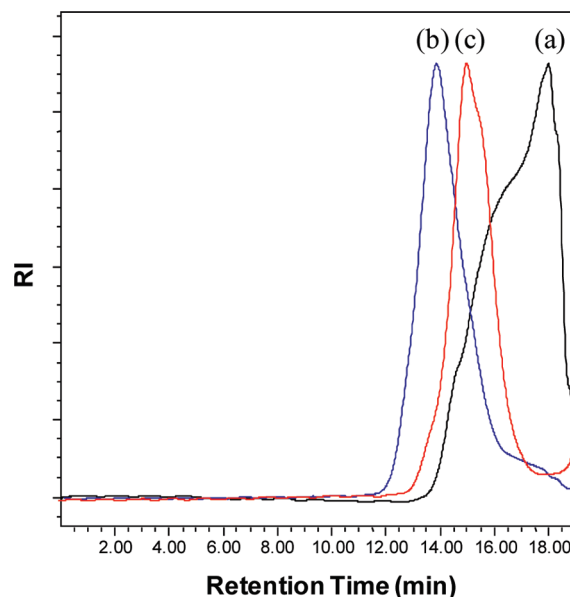


**Figure 2.** Comparison of gel permeation chromatography (GPC) traces for (a) fluorene macroinitiator, **2**, ( $M_w = 1600$  Da, PDI ( $M_w/M_n$ ) = 4.7), (b) fluorene linear precursor, **3**, ( $M_w = 143\,000$  Da, PDI ( $M_w/M_n$ ) = 2.4), and (c) fluorene nanoparticle, **4** ( $M_w = 99\,000$  Da, PDI ( $M_w/M_n$ ) = 2.0).

and  $\text{CH}_2$  from benzofluorene) 1.0–2.2 (br m, CH and  $\text{CH}_2$  from poly(styrene) backbone), 0.62–0.82 (br s,  $\text{CH}_2$  and  $\text{CH}_3$  from poly(fluorene) *n*-hexyl substituents).

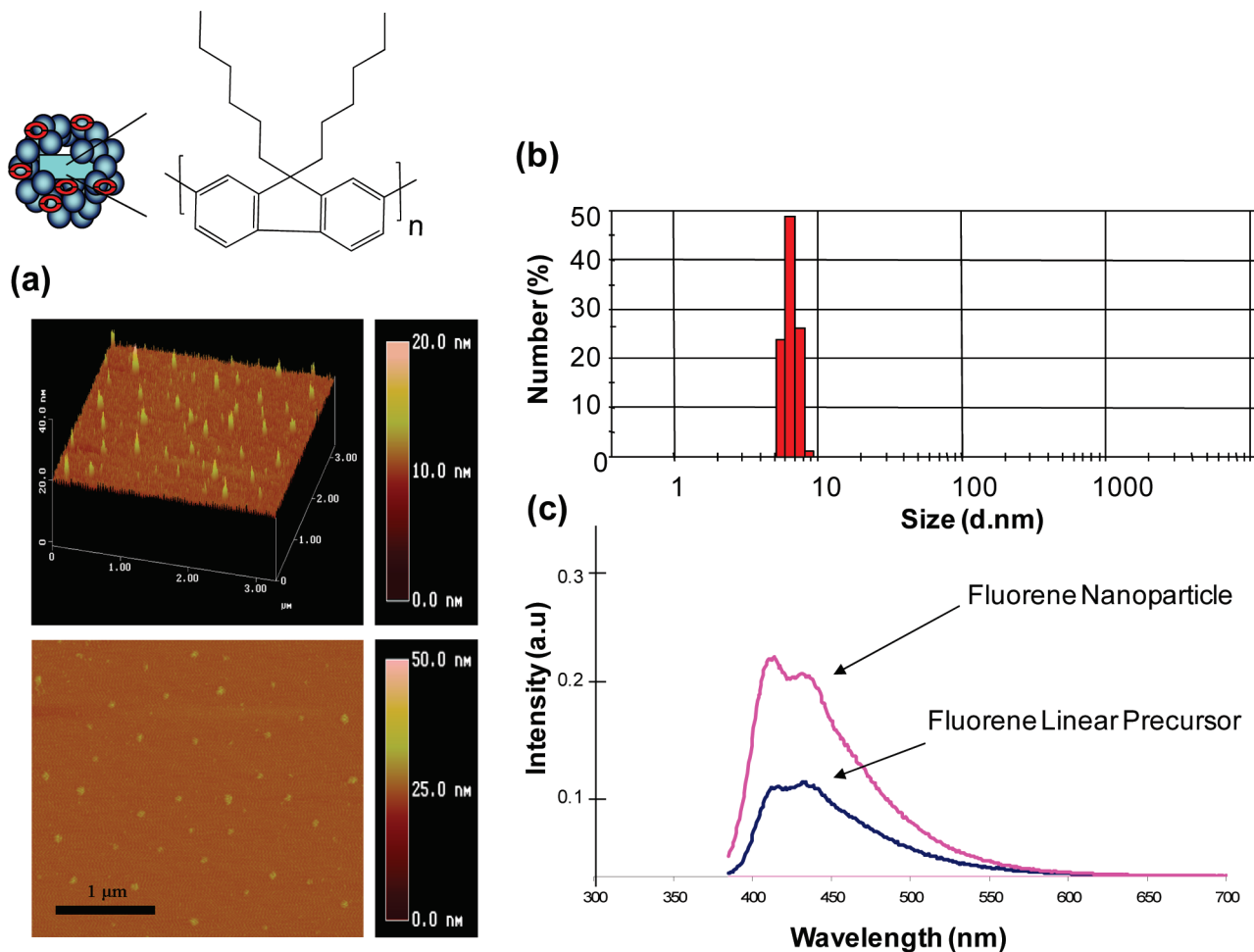


**Figure 3.** (a) Atomic force microscopy (AFM) height images of polystyrene fluorene chain collapsed nanoparticles, **4**, dispersed on silicon substrate. (b) Size distribution from dynamic light scattering (DLS) of fluorene nanoparticle, **4**, in solution ( $5 \times 10^{-3}$  mM in dichloromethane) and fluorene nanoparticle, **4**, in solution ( $5 \times 10^{-3}$  mM in dichloromethane).

**Fluorene Nanoparticle Formation, 4.** A 500 mL three-neck round-bottom flask was equipped with a condenser, an internal thermometer, and a gas inlet. Dibenzyl ether (250 mL) was added to the flask and heated to 260 °C under nitrogen. A solution of fluorene linear precursor **4** (0.30 g,  $M_w = 143\,000$  (GPC), PDI=2.4) was dissolved in 5 mL of benzyl ether and added dropwise via a peristaltic pump at 0.2 mL/min with vigorous stirring. Once all of the solution was added to the flask, the heat was removed. The solvent was distilled under reduced pressure, and the product was dissolved in dichloromethane and purified through precipitation into methanol. This gave nanoparticles in the form of a brown solid (0.25 g, 83%,  $\Phi_f = 6\%$ ,  $M_w = 99\,000$ , PDI=2.0).  $^1\text{H}$  NMR (400 MHz,  $\text{CDCl}_3$ ,  $\delta$ ): 7.45–7.65 (m, ArH from poly(fluorene)), 6.05–7.35 (m, ArH from poly(styrene) and poly(fluorene)), 2.45–2.82 (br m,  $\text{CH}_2$ ), 1.02–2.20 (m, CH and  $\text{CH}_2$  from poly(styrene) backbone), 0.62–0.82 (br s,  $\text{CH}_2$  and  $\text{CH}_3$  from poly(fluorene) *n*-hexyl substituents).

**Synthesis of 90% Fluorene/10% Thiophene Macromolecular Initiator, 5.** A 100 mL three-neck round-bottom flask containing bis(1,5-cyclooctadiene)nickel(0) (1.24 g, 4.50 mmol), 2,2'-bipyridyl (0.78 g, 5.0 mmol), dry DMF (10 mL), and dry toluene (6 mL) was heated under argon to 80 °C for 30 min. Then 2,7-dibromo-9,9'-di-*n*-hexylfluorene (0.98 g, 2.0 mmol), 2,5-dibromo-3-hexylthiophene (0.16 g, 0.50 mmol), and **1** (0.28 g, 0.70 mmol) dissolved in 6 mL of degassed toluene were added under argon to the dark blue reaction mixture. After heating for 24 h in the dark, the hot polymer solution was precipitated into 600 mL of a 1:1:1 solution of HCl: acetone:MeOH. After isolating the crude product via filtration, the bromo-substituted  $\alpha$ -alkoxyamine-capped polymer was dissolved

in dichloromethane (5 mL) and reprecipitated into a mixture of 440 mL of a acetone:MeOH solution for further purification. (0.96 g, 80.0%,  $M_w = 3800$ , PDI = 6.0).  $^1\text{H}$  NMR (400 MHz,  $\text{CDCl}_3$ ,  $\delta$ ): 7.19–7.8 (m, ArH), 2.17 (br s,  $\text{CH}_2$ ), 1.75 (m,  $\text{CH}_2$ ), 1.32 (br s,  $\text{CH}_2$ ), 1.15 (s,  $\text{CH}_2$ ), 0.85 (br s,  $\text{CH}_3$ ).  $^{13}\text{C}$  NMR (100 MHz,  $\text{CDCl}_3$ ,  $\delta$ ): 148.3, 141.0, 139.9, 138.4, 137.1, 135.1, 134.0, 133.1, 130.5, 130.1, 128.9, 126.3, 125.3, 124.7, 123.0, 122.3, 122.1, 50.3, 43.9, 40.1, 32.2, 31.8, 28.9, 24.2, 22.7, 21.6.

**90% Fluorene/10% Thiophene Linear Precursor, 6.** A mixture of **5** (0.18 g, 0.05 mmol,  $M_w = 3800$  (GPC), PDI = 6.0), styrene (1.01 g, 9.72 mmol), and vinylbenzosulfone (0.21 g, 1.08 mmol) dissolved in 1,2-dichlorobenzene (1.0 mL) was degassed by three freeze/pump/thaw cycles, sealed under argon, and heated at 124 °C for 16 h. The viscous reaction mixture was then allowed to cool, dissolved in dichloromethane (10 mL), and precipitated into methanol (1000 mL). The purified polymer was collected by vacuum filtration and dried to give the copolymer as an off-white solid (1.19 g, 85.0% yield,  $M_w = 39\,000$  (GPC), PDI=4.8,  $\Phi_f = 1.7\%$ ).  $^1\text{H}$  NMR (400 MHz,  $\text{CDCl}_3$ ,  $\delta$ ): 7.45–7.65 (m, ArH from poly(fluorene)), 6.05–7.30 (m, ArH, from poly(styrene), poly(fluorene), and poly(thiophene)), 3.97–4.30 (br m, CH and  $\text{CH}_2$  from benzosulfone), 0.85–2.1 (br m, CH and  $\text{CH}_2$  from poly(styrene) backbone), 0.70–0.85 (br s,  $\text{CH}_2$  and  $\text{CH}_3$  from poly(fluorene) *n*-hexyl substituents).

**90% Fluorene/10% Thiophene Nanoparticle Formation, 7.** Compound **7** was prepared by using a solution of 90% fluorene/10% thiophene linear precursor **6** (0.30 g,  $M_w = 39\,000$ , PDI=4.8) dissolved in 5 mL of benzyl ether following a procedure equivalent to **4** (0.23 g, 77%,  $\Phi_f = 1.8\%$ ,  $M_w = 74\,000$  (GPC), PDI=2.1).



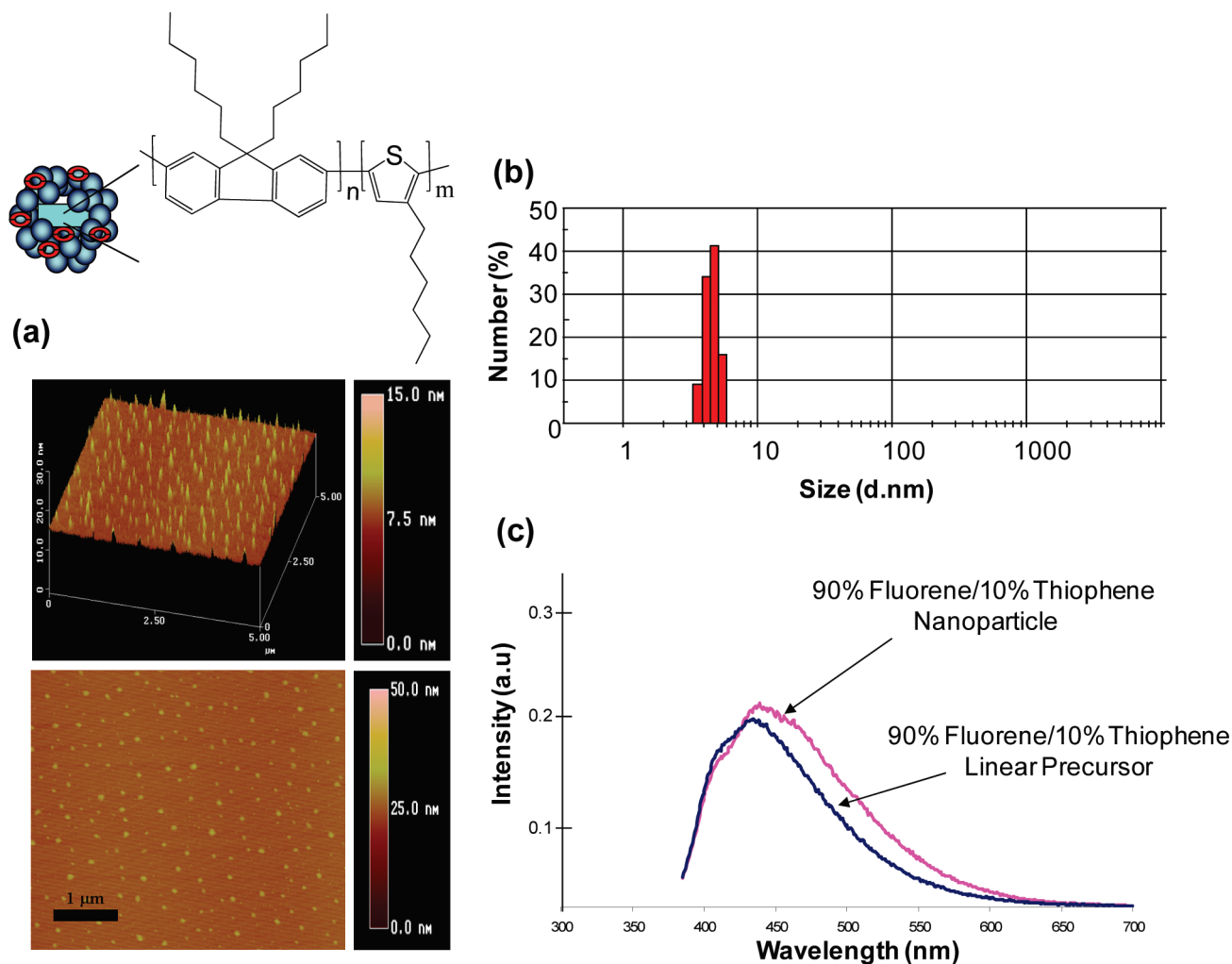


**Figure 4.** (a) Atomic force microscopy (AFM) height images of polystyrene 90% fluorene/10% thiophene chain collapsed nanoparticles, **7**, dispersed on silicon substrate. (b) Size distribution from dynamic light scattering (DLS) of 90% fluorene/10% thiophene nanoparticle, **7**. (c) Photoluminescence (PL) spectra of 90% fluorene/10% thiophene linear precursor, **6**, in solution ( $5 \times 10^{-3}$  mM in dichloromethane) and 90% fluorene/10% thiophene nanoparticle, **7**, in solution ( $5 \times 10^{-3}$  mM in dichloromethane).

$^1\text{H}$  NMR (400 MHz,  $\text{CDCl}_3$ ,  $\delta$ ): 7.55–7.65 (m, ArH from poly(fluorene)), 6.05–7.40 (m, ArH from poly(styrene), poly(fluorene) and poly(thiophene)), 2.40–2.90 (br m,  $\text{CH}_2$ ), 1.10–2.10 (m, CH and  $\text{CH}_2$  from poly(styrene) backbone), 0.60–0.85 (br s,  $\text{CH}_2$  and  $\text{CH}_3$  from poly(fluorene) *n*-hexyl substituents).

## Results and Discussion

In the design of supramolecular semiconducting nanoparticles derived from one polymer chain, we sought to synthesize ABA triblock copolymer precursors that are comprised of block copolymers (A), copolymerized from styrene and vinylbenzothiosulfone cross-linker monomers (Scheme 1), as well as a center block of fluorene and fluorene/thiophene copolymers. In our strategy, we prepared the semiconducting block (B) first in the form of a telechelic macroinitiator with both chain ends functionalized by a novel bromo-substituted  $\alpha$ -alkoxyamine living free radical initiator, **1**. While telechelic macroinitiators from conjugated polymers had been previously prepared with TEMPO derivatives as chain ends,<sup>23,24</sup> we decided to prepare a bromo-functionalized living free radical initiator to provide a greater fidelity and control of the styrene copolymers growing from the conjugated macroinitiator. Utilizing Yamamoto polymerization conditions,<sup>25</sup> dibromo derivatives of the fluorene and thiophene family are polymerized together with the prepared bromo  $\alpha$ -alkoxyamine initiator derivative, **1**, which resulted in homo- or copolymers of

fluorene and/or thiophenes. In this fashion, a fluorene B block of 6600 Da (from NMR, Table 1) molecular weight ( $M_n$ ), **2**, and a fluorene/thiophene (90/10) block with a  $M_n$  of 6700 Da (from NMR), **5**, were obtained.

To prepare suitable linear polymer precursors, these macroinitiators were polymerized with styrene and 10% vinylbenzothiosulfone cross-linker<sup>22</sup> to form ABA triblock copolymers that contain the semiconducting homo- or copolymer block as a central segment in linear styrene copolymer blocks (Scheme 1). To investigate the site isolation effects and to encapsulate the semiconducting block efficiently, we sought molecular weight ratios of nearly 10:1 or lower ratios of 5:1 of the styrene/benzothiosulfone A copolymer block to the fluorene or fluorene/thiophene center blocks. The macroinitiators were polymerized at 124 °C with 1,2-dichlorobenzene as solvent for 16 h to achieve a quantitative conversion of the oligomer mixture which was used immediately after precipitation into MeOH. As an indication of the controlled polymerizations by the macroinitiator, a significant reduction of the polydispersity of the linear precursor triblock copolymers **3** and **6** were observed. While the polydispersities for the macroinitiators **2** and **5** showed average values of 4.7 and 6.0, typical for polymerizations under Yamamoto conditions prior to purification, the living polymerization conditions could narrow the polydispersities significantly to 2.4 and 4.8 (Figures 2 and 5).<sup>26</sup> Analysis of the ABA triblock copolymers

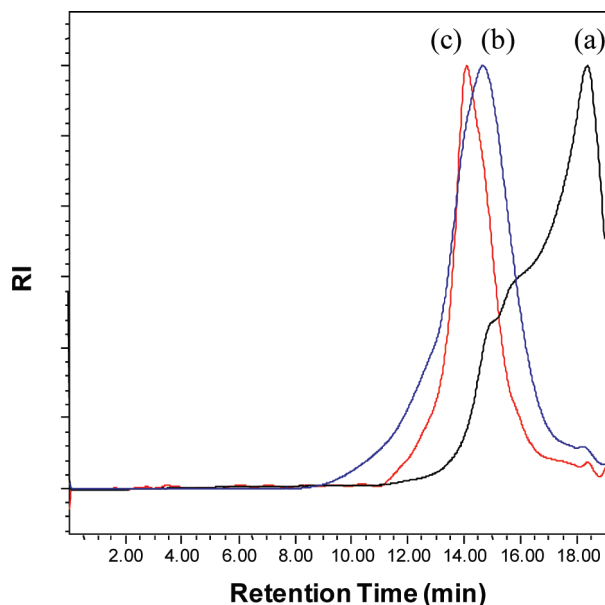


**Figure 5.** Comparison of gel permeation chromatography (GPC) traces for (a) 90% thiophene/10% fluorene macroinitiator, **5** ( $M_w = 3800$  Da, PDI ( $M_w/M_n$ ) = 6.0), (b) 90% fluorene/10% thiophene linear precursor, **6** ( $M_w = 39\,000$  Da, PDI ( $M_w/M_n$ ) = 4.8), and (c) 90% fluorene/10% thiophene nanoparticle, **7** ( $M_w = 74\,000$  Da, PDI ( $M_w/M_n$ ) = 2.1).

with NMR and GPC could further verify the influence of the molecular weight length of the polystyrene/vinylbenzocyclobutene 10% block A growth from the macroinitiator, **2**, to give the 5:1:5 and 8:1:8 molecular weight ratios of the resulting linear ABA block copolymer precursor. Interestingly, we found that linear precursor, **3**, with higher molecular weight A blocks with an 8:1:8 ratio (Table 1) showed not only the more narrowed polydispersity of 2.4, half of the original polydispersity value, but also a retention time that is in agreement with coiled polymers of the polystyrene standard. In contrast to these analytical observations, a reduction in molecular weight of about a third in the A blocks grown from fluorene/thiophene macroinitiator, **5**, to form linear precursor, **6**, with a 5:1:5 molecular weight ratio, had a significant influence, resulting in a lower reduction of the polydispersity value of a factor of 1.25 of the original value and in a reduced accuracy of the molecular weight determination by GPC with polystyrene standards. The ABA triblock copolymer **6** displayed more of the rod-coil character according to the retention time in the size exclusion chromatography and giving a lower value of the molecular weight as determined via NMR (Table 1 and Figure 5).

After both of the ABA triblock copolymers were prepared and characterized, the formation of the nanoparticles via an intramolecular chain collapse process was conducted. During this process, the benzosulfone functionality, as part of the A block copolymer, forms reactive *o*-quinodimethane intermediates to react as stable benzocyclooctadiene cross-linked entities, equivalent to products observed with benzocyclobutene derivatives.<sup>22,27</sup> The characterization of the produced particles **4** and **7** indicated that during the cross-linking event the semiconducting block does not participate in the reaction process. Analysis with  $^1\text{H}$  NMR spectroscopy further verified a successful intramolecular chain collapse process with the disappearance of the characteristic protons of the benzosulfone ring at 4.0–4.3 ppm in the linear precursor to be replaced by the protons at 2.6–3.1 ppm that are observed with the appearance of benzocyclooctadiene units in the nanostructure (Figure 1). Additionally, no broadening of the spectra was detected as a typical attribute to successful intramolecular chain collapse process that has been demonstrated in

several examples in comparable reactions with homopolymers from polystyrene<sup>27</sup> and poly(benzyl acrylates).<sup>22</sup>

Another measure that is used to test the control over the intramolecular chain collapse process is the analysis of the soluble products in size exclusion chromatography (GPC). The proposed change in conformation is typically detected by a change in the hydrodynamic volume that results in a reduced molecular weight of the nanoparticle,<sup>27</sup> in contrast to the precursor being measured, and also a narrowing of the polydispersity index (PDI) can be obtained. The products from the intramolecular chain collapse process, **4**, derived from the block copolymers with the polyfluorene as the center block correspond to this previously investigated behavior as a response to the change in conformation with a shift to lower retention times and narrowed polydispersity index of 2.0 (Figure 2). To complete the analysis, dynamic light scattering (DLS) and atomic force microscopy (AFM) could confirm nanoparticle formation to achieve particles of 5–10 nm (Figure 3).

In the same course of analysis, the second set of particles, **7**, from the block copolymer with the thiophene/fluorene as center block was investigated. Here, the change in hydrodynamic volume of the nanoparticle could not be followed by GPC because the retention time of the linear precursor **6** could not be used as an analytical tool to evaluate the change in the conformation. As described earlier, the rod-coil behavior of the triblock copolymer precursor, **6**, does not respond well to the polystyrene standard and detects an already lower molecular weight than actually determined via NMR. Therefore, we compared the nanoparticle traces of **7** with polystyrene standards of the same molecular weight as of the ABA block copolymer precursors determined by NMR of 70 K and the shift to lower molecular weight of the nanoparticles through the change in the hydrodynamic volume could be verified. Additionally, we also observed a significantly narrowed polydispersity index of 2.1, in contrast to the ABA block copolymer before chain collapse. The AFM and DLS data could support the proposed controlled nanoparticle formation from the intramolecular chain collapse process and particles in the range of 3–7 nm were detected (Figure 4).

Furthermore, to evaluate the effect of the architectural change in the electrooptical properties of the embedded conjugated polymer center core, we measured the change of the photoluminescence intensities of the nanoparticles compared to their linear precursors in solution. We found that the quantum efficiency of nanoparticles with a value of 6%, with the block copolymer weight ratio of 8:1:8, was 3 times higher as compared to the linear precursor, **3**, with a measured value of 2%. To determine any solvent dependence of the quantum efficiency values, we performed the measurements both in dichloromethane and in cyclohexane, but we detected no difference in the quantum efficiency values. Furthermore, we could demonstrate that the molecular weight ratio of the block copolymers had a major effect on the encapsulation efficiencies of the conducting polymer block. With the reduction of the A block copolymer of about 1.6, a third of the total molecular weight, the photoluminescence intensity and quantum efficiencies of the nanoparticles, **7**, with a value of 1.8% were not very different compared to the linear precursor (1.7%). Therefore, we could conclude that the 5:1:5 molecular weight ratios were not sufficient to achieve a complete encapsulation of the conducting polymer block copolymer to result in a significant change in the quantum efficiencies of the nanoparticles. With this study, we could evaluate the ideal molecular weight ratios as parameters to design future ABA triblock compositions to afford site isolation of a conducting center block copolymer that leads to an increase in photoluminescence of nanoparticles derived from intramolecular chain collapse processes.

## Conclusions

We report a synthesis pathway that yields nanoparticles with single conducting polymers embedded in polystyrene in the size dimension of 5–10 nm. The key step in this synthesis is the intramolecular chain collapse of an ABA triblock copolymer, comprised from polystyrene A blocks and a conducting polymer as B block. To facilitate an intramolecular chain collapse with the intent to site isolate or embed the conducting polymer, the styrene block was copolymerized with 10% of vinylbenzosulfone from macroinitiators of fluorene homopolymers and fluorene/thiophene copolymers under nitroxide-mediated living free polymerization conditions. AFM and DLS studies confirmed the formation of nanoparticles through the chain collapse process of individual ABA triblock copolymer chains. The molecular weight ratios of the A block to the B blocks were varied to investigate the effect of site isolation of the center block in photoluminescence studies once the particles were formed. We found that a ratio of nearly 10:1 achieves a 3-fold increase of quantum efficiency, whereas a ratio of 5:1 accomplishes only a slight increase in quantum efficiency of the final nanoparticles.

**Acknowledgment.** E.H. gratefully acknowledges financial support from the CAREER program of the National Science Foundation under Award CH-0645737. C.T.A. was supported by a Chemistry-Biology Interface Program Fellowship under a NIH Training Grant T32 GM065086-5 and an ACS PRF Grant 46620-G7. The authors also thank Vanderbilt University (VINSE, Vanderbilt Institute of Nanoscale and Engineering) for supporting this research.

## References and Notes

- (1) Bhaviripudi, S.; Qi, J.; Hu, E. L.; Belcher, A. M. *Nano Lett.* **2007**, 7 (11), 3512–3517.
- (2) Mao, C. B.; Qi, J. F.; Belcher, A. M. *Adv. Funct. Mater.* **2003**, 13 (8), 648–656.
- (3) Guldi, D. M.; Rahman, G. M. A.; Sgobba, V.; Kotov, N. A.; Bonifazi, D.; Prato, M. *J. Am. Chem. Soc.* **2006**, 128 (7), 2315–2323.
- (4) Jain, K. K. *Expert Rev. Mol. Diagn.* **2003**, 3 (2), 153–161.
- (5) Kricka, L. J. *Ann. Clin. Biochem.* **2002**, 39, 114–129.
- (6) Ng, B. C.; Yu, M.; Gopal, A.; Rome, L. H.; Monbouquette, H. G.; Tolbert, S. H. *Nano Lett.* **2008**, 8 (10), 3503–3509.
- (7) You, C. C.; Miranda, O. R.; Gider, B.; Ghosh, P. S.; Kim, I. B.; Erdogan, B.; Krovi, S. A.; Bunz, U. H. F.; Rotello, V. M. *Nat. Nanotechnol.* **2007**, 2 (5), 318–323.
- (8) Almutairi, A.; Akers, W. J.; Berezin, M. Y.; Achilefu, S.; Frechet, J. M. J. *Mol. Pharmaceutics* **2008**, 5 (6), 1103–1110.
- (9) Kim, J. H.; Park, K.; Nam, H. Y.; Lee, S.; Kim, K.; Kwon, I. C. *Prog. Polym. Sci.* **2007**, 32 (8–9), 1031–1053.
- (10) Morales, A. R.; Schafer-Hales, K. J.; Marcus, A. I.; Belfield, K. D. *Bioconjugate Chem.* **2008**, 19 (12), 2559–2567.
- (11) Mcrae, R. L.; Phillips, R. L.; Kim, I. B.; Bunz, U. H. F.; Fahrni, C. J. *J. Am. Chem. Soc.* **2008**, 130 (25), 7851–7853.
- (12) Kohl, C.; Weil, T.; Qu, J. Q.; Mullen, K. *Chem.—Eur. J.* **2004**, 10 (21), 5297–5310.
- (13) Yin, M.; Shen, J.; Pflugfelder, G. O.; Mullen, K. *J. Am. Chem. Soc.* **2008**, 130 (25), 7806–7809.
- (14) Burns, A. A.; Vider, J.; Ow, H.; Herz, E.; Penate-Medina, O.; Baumgart, M.; Larson, S. M.; Wiesner, U.; Bradbury, M. *Nano Lett.* **2009**, 9 (1), 442–448.
- (15) Burns, A.; Sengupta, P.; Zedayko, T.; Baird, B.; Wiesner, U. *Small* **2006**, 2 (6), 723–726.
- (16) Kietzke, T.; Stiller, B.; Landfester, K.; Montenegro, R.; Neher, D. *Synth. Met.* **2005**, 152 (1–3), 101–104.
- (17) Landfester, K.; Montenegro, R.; Scherf, U.; Guntner, R.; Asawapirom, U.; Patil, S.; Neher, D.; Kietzke, T. *Adv. Mater.* **2002**, 14 (9), 651–655.
- (18) Wu, C.; Bull, B.; Szymanski, C.; Christensen, K.; McNeill, J. *ACS Nano* **2008**, 2 (11), 2415–2423.
- (19) Wu, C. F.; Szymanski, C.; McNeill, J. *Langmuir* **2006**, 22 (7), 2956–2960.
- (20) Palacios, R. E.; Fan, F. R. F.; Grey, J. K.; Suk, J.; Bard, A. J.; Barbara, P. F. *Nat. Mater.* **2007**, 6 (9), 680–685.
- (21) Benoit, D.; Chaplinski, V.; Braslau, R.; Hawker, C. J. *J. Am. Chem. Soc.* **1999**, 121 (16), 3904–3920.
- (22) Croce, T. A.; Hamilton, S. K.; Chen, M. L.; Muchalski, H.; Harth, E. *Macromolecules* **2007**, 40 (17), 6028–6031.
- (23) Hawker, C. J.; Klaerner, G.; Lee, J.; Lee, V.; Miller, R. D.; Scott, J. C. U.S. Patent 6,355,756, **2002**.
- (24) Hawker, C. J.; Bosman, A. W.; Harth, E. *Chem. Rev.* **2001**, 101 (12), 3661–3688.
- (25) Yamamoto, T.; Morita, A.; Miyazaki, Y.; Maruyama, T.; Wakayama, H.; Zhou, Z.; Nakamura, Y.; Kanbara, T.; Sasaki, S.; Kubota, K. *Macromolecules* **1992**, 25 (4), 1214–1223.
- (26) Klaerner, G.; Miller, R. D. *Macromolecules* **1998**, 31 (6), 2007–2009.
- (27) Harth, E.; Van Horn, B.; Lee, V. Y.; Germack, D. S.; Gonzales, C. P.; Miller, R. D.; Hawker, C. J. *J. Am. Chem. Soc.* **2002**, 124 (29), 8653–8660.